FOR THE RECORD

Assignment-free solution NMR method reveals CesT as an unswapped homodimer

SIGRUN RUMPEL, RAGHAVENDRAN LAKSHMI, STEFAN BECKER, AND MARKUS ZWECKSTETTER

Department for NMR-Based Structural Biology, Max Planck Institute for Biophysical Chemistry, 37077 Göttingen, Germany

(RECEIVED April 30, 2008; FINAL REVISION July 17, 2008; ACCEPTED July 24, 2008)

Abstract

The X-ray structure of the homodimeric chaperone CesT is the only structure among the type three secretion system (TTSS) chaperones that shows a domain swap. This swap has potential importance for the mechanism of effector translocation through a TTSS. Here we present two nuclear magnetic resonance strategies exploiting pre-existing structural models and residual dipolar couplings (RDCs), which reveal the unswapped 35.4-kDa dimer to be present in solution. Particularly efficient is the discrimination of a swapped and unswapped structural state performed simultaneously to automatic backbone assignment using only HN-RDCs and carbonyl backbone chemical shifts. This direct approach may prove to be generally useful to rapidly differentiate two structural models.

Keywords: domain swap; residual dipolar couplings; PALES; charge-shape prediction; MARS

Three-dimensional (3D) domain swapping is defined as the replacement of a portion of the tertiary structure of a protein with an identical structural element from a second protein molecule (Bennett et al. 1995). The structurally characterized domain-swapped proteins and their variety of functions were reviewed by Liu and Eisenberg (2002). As 3D domain swapping can serve as a mechanism for reversible oligomerization and is implicated in amyloidosis, it has gained recent interest (Bennett et al. 2006). However, its biological effect on protein function is not understood.

The 156-residue chaperone CesT belongs to the family of type three secretion system (TTSS) chaperones that form homodimers. CesT is involved in the secretion process of effector proteins from the cytoplasm of the human pathogens enteropathogenic (EPEC) and enterohemorrhagic (EHEC) *Escherichia coli* into the eukaryotic cell (Garmendia et al. 2005). The crystal structure of CesT from EHEC O157:H7 reveals a domain-swapped homodimer, the first 34 N- and the last 18 C-terminal residues being intertwined with the adjacent monomer (Fig. 1A). The absence of this domain swap in all other known crystal structures of TTSS chaperones raises the question of its biological function. On the basis of structural homology with the other known TTSS chaperone structures, an unswapped model structure of CesT was constructed (Fig. 1B; Luo et al. 2001). Its dimer interface has only half the size of the interface of the swapped CesT dimer. Yet only the unswapped structure is consistent with the surfaces identified as important for effector-binding in known structures of homologous chaperone/effector complexes (Lilic et al. 2006). In addition to the domain-swapped structure of CesT, a domain swap was reported for the chaperone-binding domain of the effector YopH and an intermolecular crossover for the SptP/SipP chaperone/effector complex (Stebbins and Galan 2001). Thus, domain swapping may play a role for the dissociation of the effector from its chaperone, and further structural data providing insight into the domain swapping capability of TTSS chaperons are required.

Reprint requests to: Markus Zweckstetter, NMR-based Structural Biology, Max Planck Institute for Biophysical Chemistry, Am Fassberg 11, D-37077 Göttingen, Germany; e-mail: mzwecks@gwdg.de; fax: 49-551-201-2202.

Article and publication are at http://www.proteinscience.org/cgi/doi/10.1110/ps.036160.108.

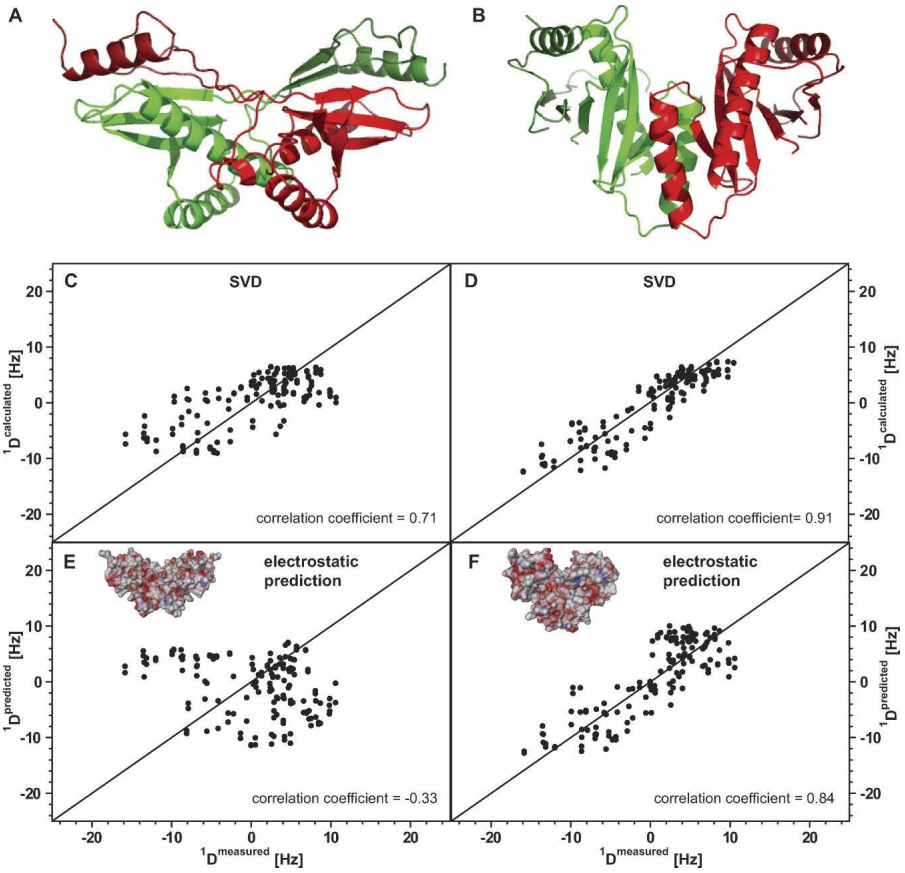

Figure 1. Ribbon presentations looking at the dimer twofold axis of the X-ray (*A*) and model structure (*B*) of CesT. (*C–F*) Correlation between experimental and back-calculated (*C*,*D*) or charge-shape predicted HN-RDCs (*E*,*F*) for the X-ray (*C*,*E*) and the model structure (*D*,*F*) of CesT. The *insets* in *E* and *F* show the electrostatic surface of the X-ray and model structure of CesT, respectively (positive and negative potentials colored blue and red).

The long-range orientational information provided by residual dipolar couplings (RDCs) renders them valuable in the determination of the assembly of monomers within a macromolecular complex and to derive relative domain orientations, for example, in a domain-swapped dimer (Clore and Bewley 2002). RDCs can be predicted from a known 3D structure with the software PALES (Zweckstetter 2008), which uses a simplified simulation method that takes into account the shape and charge distribution of the protein's structure and the surface charge of the alignment medium (Zweckstetter et al. 2004). This method allows the distinction between the parallel and antiparallel arrangement of coiled-coil homodimers, which have a very similar shape but different charge distribution (Schnell et al. 2005; Zweckstetter et al. 2005) and to identify a near-native docking model (Rumpel et al. 2008).

Here, we investigated whether the TTSS chaperone CesT is present in its domain-swapped or unswapped state in solution to better understand the intriguing occurrence of domain swap for TTSS components. Two approaches reveal the unswapped chaperone to be present in solution: (1) the correlation between assigned and charge-shape predicted RDCs and (2) the number of reliable assignments obtained with the software MARS, which performs simultaneously the charge-shape prediction and the automatic backbone assignment based on experimental chemical shifts and RDCs. Depending on the differences in the surface charge distribution, both approaches can also be used to distinguish other swapped and unswapped structures. They may prove to be an important tool for determining the effector translocation via a TTSS.

Results and Discussion

The X-ray and model structure used to investigate the solution structure of CesT from EPEC O127:H6 were generated as described in Materials and Methods. In the unswapped monomer all strands form an antiparallel β-sheet, whereas in the swapped monomer the first helix and strand as well as the last strand are rotated outward through a conformational change of residue 35 and

residues 129–138. Different structural elements of the swapped and unswapped monomer constitute the homodimer interface of the CesT X-ray and model structure, respectively. Both interfaces occur in the CesT crystal (Luo et al. 2001) and result in a different shape and surface charge distribution (Fig. 1E,F, insets). The model structure of CesT is the structure that is similar to the known structures of homologues TTSS chaperones and that contains the surfaces identified as important for effector-binding (Lilic et al. 2006).

Seventy-five nonoverlapping HN-RDCs could be determined accurately from a two-dimensional (2D) IPAP-$^{1}H^{15}N$ HSQC for the 35.4-kDa CesT dimer. Using a 3D TROSY-HNCO and a 3D TROSY-HN(CO)CA, 75 C′N- and 51 C′Cα-RDCs were determined, and the number of HN-RDCs was increased to 100. Experimental RDCs were best-fit to the X-ray and the model structure of CesT using singular value decomposition (Losonczi et al. 1999) as implemented in PALES (Zweckstetter 2008). Using only a monomeric subunit of each structure and the HN-RDCs from the 2D IPAP-$^{1}H^{15}N$ HSQC, the resulting Pearson's correlation coefficients r between experimental and back-calculated RDCs were 0.85 ($r = 0.79$, all experimental RDCs) and 0.93 ($r = 0.93$, all experimental RDCs) for the X-ray and model structure, respectively. Best-fitting the 75 HN-RDCs from the 2D IPAP-$^{1}H^{15}N$ HSQC to the full dimeric arrangement of the model or the X-ray structure, r was 0.91 and 0.71, respectively (Fig. 1C,D). Using all 226 RDCs, the correlation coefficients were 0.93 and 0.71, respectively. The alignment tensor that was back-calculated from the model structure was close to axially symmetric (rhombicity $R = 0.15$) and had an alignment magnitude $D_a(NH)$ of -6.2 Hz, whereas the alignment tensor back-calculated from the X-ray structure was more rhombic ($R = 0.29$) with a $D_a(NH)$ of -4.5 Hz. Thus, best-fitting of RDCs pointed to the unswapped model structure as the structure present under solution NMR conditions.

To obtain further evidence for the presence of the unswapped conformation of CesT in solution, RDCs were predicted for both CesT structures using the electrostatic module of PALES (Zweckstetter et al. 2004). In Figure 1, E and F, RDCs predicted for the two structures by PALES are compared with the 75 experimental HN-RDCs extracted from the 2D IPAP-$^{1}H^{15}N$ HSQC. For the X-ray structure there is no correlation between predicted and experimental values ($r = -0.33$, Fig. 1F). In contrast, the sign and size of the predicted and experimental RDCs fit very well to the model structure ($r = 0.84$, Fig. 1F). Using all 226 experimental RDCs, r was -0.15 and 0.89 for the X-ray and model structure, respectively. Consequently, an unswapped conformation, which is best represented by the model structure, exists under solution NMR conditions.

To further speed up the distinction between a swapped and unswapped structure, the feasibility of discriminating the two structures of CesT without prior time-consuming backbone assignment was tested. The easiest way would be to compare R and D_a, as determined from the experimental RDC distribution (Clore et al. 1998), with those for the charge-shape predicted RDCs from both structures. However, D_a and R derived from the model and X-ray structures of CesT did not differ sufficiently (taking into account the accuracy with which these values can be determined from the histogram of RDCs and the accuracy of the PALES prediction) to reliably discriminate the two structures (data not shown).

Good progress has been made with approaches that aim at automation of backbone assignment (Baran et al. 2004). Moreover, the program MARS is able to use RDCs calculated from a 3D structure in the assignment process (Jung and Zweckstetter 2004b). We tested whether it is possible to efficiently discriminate between the swapped and unswapped structure of the 35.4-kDa CesT dimer by a combined MARS–PALES approach: RDCs predicted from the shape and charge distribution by PALES are used to enhance automatic backbone assignment by MARS. For distinction, we used the number of reliable assignments obtained by MARS (Table 1). To automatically assign more than 50% of backbone resonances, at least one type of connectivity information was required. On the other hand, when discrimination between two structures is the primary aim, combination of a single type of carbon chemical shift (e.g., C'_{i-1}) with one type of RDC (e.g., $^{1}D_{NH}$) was sufficient. With 68 more reliable assignments for the model than for the X-ray structure, the largest difference in reliable assignments was obtained for HN- and NC′-RDCs in combination with C_α and $C_{\alpha-1}$ chemical shifts. Our tests reveal that the distinction between the swapped and unswapped dimer using a combined MARS–PALES approach is highly reliable. This opens up the way to efficiently investigate the presence of domain swaps in large dimeric proteins that are not accessible to a conventional structure determination. C'_{i-1} chemical shifts may be measured using a 3D HNCO, and HN-RDCs can be obtained from a 2D IPAP-HSQC under isotropic and anisotropic conditions. Alternatively, a 3D HNCA, which is a bit less sensitive than the HNCO but also provides connectivity information, might be useful. When only ^{15}N-labeling of the protein is possible, HNCA and HNCO spectra might also be recorded with ^{13}C at natural abundance (Kupce et al. 2003). Using the outlined approach, the domain-swapped structure of CesT, which is potentially important for the dissociation of its effectors during secretion, may be revealed when changing the solution conditions. Lowering the pH and/or increasing the salt concentration might induce the domain swap as CesT was crystallized at

Table 1. *MARS output for the model and X-ray structure obtained with different sets of RDCs and chemical shifts*

Experimental input data		No. of assignments out of 141[a]							
		Model			X-ray				
RDCs	Chemical shifts[b]	Total assigned[c]	Reliable[d]	Wrong reliable[e]	Total assigned	Reliable	Wrong reliable	Distinction in reliable assignments[f]	
$^1D_{NH}$, $^1D_{C'C\alpha}$, $^1D_{NC'}$	C'_{i-1}, C^{α}_{i-1}, C^{β}_{i-1}, C'_i, C^{α}_i, C^{β}_i	136	127	2	102	74	0	**53**	1.7
$^1D_{NH}$, $^1D_{C'C\alpha}$, $^1D_{NC'}$	C^{α}_{i-1}, C^{β}_{i-1}, C^{α}_i, C^{β}_i	129	124	2	86	63	0	**61**	2.0
$^1D_{NH}$, $^1D_{C'C\alpha}$, $^1D_{NC'}$	C^{α}_{i-1}, C^{α}_i	120	74	2	36	15	1	**59**	4.9
$^1D_{NH}$, $^1D_{NC'}$	C^{α}_{i-1}, C^{α}_i	129	85	2	35	17	1	**68**	5.0
$^1D_{NH}$	C^{α}_{i-1}, C^{α}_i	105	82	2	50	28	7	**54**	2.9
$^1D_{NH}$	C'_{i-1}, C^{α}_{i-1}, C^{β}_{i-1}, C'_i, C^{α}_i, C^{β}_i	120	102	0	110	72	8	**30**	1.4
$^1D_{NH}$	C'_{i-1}	39	28	0	31	15	0	**13**	1.9
$^1D_{NH}$, $^1D_{C'C\alpha}$	C'_{i-1}	40	29	0	30	20	2	**9**	1.5
–	C'_{i-1}	23	19	0	21	18	1	**1**	1.0
–	C^{α}_{i-1}, C^{α}_i	110	82	0	112	75	6	**7**	1.0

[a] Number of assignable residues (total number of residues except prolines, the N-terminal residue, and residues not present in the X-ray structure).
[b] In addition to the mentioned data, N_i and HN_i chemical shifts were used.
[c] Total number of assigned residues as found in the MARS output file assignment_AA.out. These assignments were not subjected to a reliability test.
[d] Total number of high and medium reliable assignments obtained by MARS.
[e] Number of high and medium reliable assignments obtained by MARS that did not agree with the subsequent manual assignment.
[f] Difference and ratio of the number of reliable assignments that were obtained by MARS for the two structures.

pH 5.6 and 1.5 M ammonium sulfate, whereas the solution NMR experiments in this study were undertaken at pH 6.8 at 0.1 M NaCl.

The electrostatic properties of a molecule's surface are likely to change dramatically even when only small domains are swapped. Thus, identification of domain swaps using charge-shape predicted RDCs is expected to be applicable in many cases. Notably, with increasing size of the molecule and therefore an increasing number of charged residues, inaccuracies in the exact position of single charges have less influence on the overall electrostatic properties of the molecule. Therefore, charge-shape prediction of RDCs and thus identification of domain swaps is not expected to deteriorate for larger molecular weights, despite the fact that on average more side chains will be ill-defined in X-ray structures. Charge-shape prediction of RDCs might also be useful for obtaining insight into the early stages of protein aggregation, in which domain-swapped states play important roles (Eakin et al. 2006).

Materials and Methods

NMR spectroscopy

Details of sample preparation have been described elsewhere (Rumpel et al. 2005). After isotropic data collection, the ~0.5 mM CesT sample was aligned by addition of Pf1 bacteriophage to a concentration of 10 mg/mL (Hansen et al. 1998; Zweckstetter and Bax 2001). All NMR experiments were acquired at 303 K on Bruker 600, 700, or 800 spectrometers. RDCs ($^1D_{HN}$, $^1D_{NC'}$, and $^1D_{C'C\alpha}$) were gained from the difference between the J-couplings measured in the anisotropic and isotropic media. $^1J_{HN}$-couplings were determined using a 2D IPAP-$^1H^{15}N$ HSQC (Ottiger et al. 1998), $^1J_{HN}$- and $^1J_{NC'}$-couplings were measured simultaneously from three interleaved 3D TROSY-HNCO spectra (Chou et al. 2000), and $^1J_{C'C\alpha}$ was obtained from two interleaved 3D TROSY-HN(CO)CA spectra (Jaroniec et al. 2004). All spectra were processed and analyzed using NMRPipe/NMRDraw (Delaglio et al. 1995). Reported backbone assignments of CesT were used (BioMagResBank accession number 6451).

Generation of the unswapped homodimer structure of CesT

To generate the model structure of CesT the pdb entry 1K3E for CesT was used. This entry contains the coordinates for the crystallographic dimer of CesT with the dimer interface corresponding to the homologue chaperones as well as the symmetry transformations to produce the crystallographically related molecules. The symmetry transformations to obtain the noncrystallographic dimer were performed with Coot (Emsley and Cowtan 2004). From this X-ray structure of CesT, the nonswapped monomer was generated by changing the chain ID of residues 1–35 and 129–146 of monomer A to B and vice versa. The resulting unswapped monomers A and B were superimposed on residues 36–128 of the crystallographic dimer of monomer A and B, respectively, to obtain the model structure of CesT. For both, model and X-ray structure of CesT, side chains of residues not present in one of the subunits were added by using the side chain of the corresponding residues of the other subunit.

Homodimer distinction using RDCs based on a known backbone assignment

RDCs were best-fit to the X-ray and model structure of CesT using singular value decomposition as implemented in PALES

(Zweckstetter 2008). RDCs were predicted for both structures based on their charge and shape with the electrostatic module of PALES (Zweckstetter et al. 2004). The default charge was attached to all ionizable residues, the Pf1 concentration was set to 10 mg/mL, and the ionic strength was adjusted to 0.1 M NaCl.

Simultaneous backbone assignment and homodimer distinction

The model and X-ray structure of CesT and different sets of experimental RDCs and chemical shifts were used as input for the automatic backbone assignment program MARS (Jung and Zweckstetter 2004a,b). During the MARS assignment process, experimental RDCs were compared with RDCs predicted for the corresponding structure. For prediction of RDCs, the magnitude and rhombicity of the alignment tensor were set to the values obtained by an analysis of the distribution of experimental RDCs (Clore et al. 1998). The orientation of the alignment tensor, on the other hand, was taken from the charge-shape prediction of molecular alignment using the electrostatic module of PALES (Zweckstetter et al. 2004). In addition, default chemical shifts employed by MARS for matching assignment fragments to the primary sequence (Jung and Zweckstetter 2004a) were replaced by chemical shifts predicted from the corresponding 3D structure (i.e., either X-ray or model structure) using the program SPARTA (Shen and Bax 2007). Mapping of chemical shifts predicted from a 3D structure improves the overall assignment quality. Differences in the number of reliable assignments obtained by MARS for the two structures (i.e., swapped X-ray structure and unswapped model structure) were used for identification of the conformation present in solution.

Acknowledgments

We thank Christian Griesinger for useful discussions. This work was supported by the Max Planck Society and a DFG Heisenberg grant (ZW71/2.1-3.1) to M.Z.

References

Baran, M.C., Huang, Y.J., Moseley, H.N., and Montelione, G.T. 2004. Automated analysis of protein NMR assignments and structures. *Chem. Rev.* **104:** 3541–3556.

Bennett, M.J., Schlunegger, M.P., and Eisenberg, D. 1995. 3D domain swapping: A mechanism for oligomer assembly. *Protein Sci.* **4:** 2455–2468.

Bennett, M.J., Sawaya, M.R., and Eisenberg, D. 2006. Deposition diseases and 3D domain swapping. *Structure* **14:** 811–824.

Chou, J.J., Delaglio, F., and Bax, A. 2000. Measurement of one-bond ^{15}N-$^{13}C'$ dipolar couplings in medium sized proteins. *J. Biomol. NMR* **18:** 101–105.

Clore, G.M. and Bewley, C.A. 2002. Using conjoined rigid body/torsion angle simulated annealing to determine the relative orientation of covalently linked protein domains from dipolar couplings. *J. Magn. Reson.* **154:** 329–335.

Clore, G.M., Gronenborn, A.M., and Bax, A. 1998. A robust method for determining magnitude of the fully asymmetric alignment tensor of oriented macromolecules in the absence of structural information. *J. Magn. Reson.* **133:** 216–221.

Delaglio, F., Grzesiek, S., Vuister, G.W., Zhu, G., Pfeifer, J., and Bax, A. 1995. NMRPipe—a multidimensional spectral processing system based on Unix pipes. *J. Biomol. NMR* **6:** 277–293.

Eakin, C.M., Berman, A.J., and Miranker, A.D. 2006. A native to amyloidogenic transition regulated by a backbone trigger. *Nat. Struct. Mol. Biol.* **13:** 202–208.

Emsley, P. and Cowtan, K. 2004. Coot: Model-building tools for molecular graphics. *Acta Crystallogr. Sect. D Biol. Crystallogr.* **60:** 2126–2132.

Garmendia, J., Frankel, G., and Crepin, V.F. 2005. Enteropathogenic and enterohemorrhagic *Escherichia coli* infections: Translocation, translocation, translocation. *Infect. Immun.* **73:** 2573–2585.

Hansen, M.R., Mueller, L., and Pardi, A. 1998. Tunable alignment of macromolecules by filamentous phage yields dipolar coupling interactions. *Nat. Struct. Biol.* **5:** 1065–1074.

Jaroniec, C.P., Ulmer, T.S., and Bax, A. 2004. Quantitative J correlation methods for the accurate measurement of $^{13}C'$-$^{13}C_{\alpha}$ dipolar couplings in proteins. *J. Biomol. NMR* **30:** 181–194.

Jung, Y.S. and Zweckstetter, M. 2004a. Mars–robust automatic backbone assignment of proteins. *J. Biomol. NMR* **30:** 11–23.

Jung, Y.S. and Zweckstetter, M. 2004b. Backbone assignment of proteins with known structure using residual dipolar couplings. *J. Biomol. NMR* **30:** 25–35.

Kupce, E., Muhandiram, D.R., and Kay, L.E. 2003. A combined HNCA/HNCO experiment for ^{15}N labeled proteins with ^{13}C at natural abundance. *J. Biomol. NMR* **27:** 175–179.

Lilic, M., Vujanac, M., and Stebbins, C.E. 2006. A common structural motif in the binding of virulence factors to bacterial secretion chaperones. *Mol. Cell* **21:** 653–664.

Liu, Y. and Eisenberg, D. 2002. 3D domain swapping: As domains continue to swap. *Protein Sci.* **11:** 1285–1299.

Losonczi, J.A., Andrec, M., Fischer, M.W., and Prestegard, J.H. 1999. Order matrix analysis of residual dipolar couplings using singular value decomposition. *J. Magn. Reson.* **138:** 334–342.

Luo, Y., Bertero, M.G., Frey, E.A., Pfuetzner, R.A., Wenk, M.R., Creagh, L., Marcus, S.L., Lim, D., Sicheri, F., Kay, C., et al. 2001. Structural and biochemical characterization of the type III secretion chaperones CesT and SigE. *Nat. Struct. Biol.* **8:** 1031–1036.

Ottiger, M., Delaglio, F., and Bax, A. 1998. Measurement of J and dipolar couplings from simplified two-dimensional NMR spectra. *J. Magn. Reson.* **131:** 373–378.

Rumpel, S., Kim, H.Y., Viyajan, V., Becker, S., and Zweckstetter, M. 2005. Letter to the Editor: Backbone resonance assignment of the homodimeric, 35 kDa chaperone CesT from enteropathogenic *Escherichia coli*. *J. Biomol. NMR* **31:** 377–378.

Rumpel, S., Becker, S., and Zweckstetter, M. 2008. High-resolution structure determination of the CylR2 homodimer using paramagnetic relaxation enhancement and structure-based prediction of molecular alignment. *J. Biomol. NMR* **40:** 1–13.

Schnell, J.R., Zhou, G.P., Zweckstetter, M., Rigby, A.C., and Chou, J.J. 2005. Rapid and accurate structure determination of coiled-coil domains using NMR dipolar couplings: Application to cGMP-dependent protein kinase Iα. *Protein Sci.* **14:** 2421–2428.

Shen, Y. and Bax, A. 2007. Protein backbone chemical shifts predicted from searching a database for torsion angle and sequence homology. *J. Biomol. NMR* **38:** 289–302.

Stebbins, C.E. and Galan, J.E. 2001. Maintenance of an unfolded polypeptide by a cognate chaperone in bacterial type III secretion. *Nature* **414:** 77–81.

Zweckstetter, M. 2008. NMR: Prediction of molecular alignment from structure using the PALES software. *Nat. Protoc.* **3:** 679–690.

Zweckstetter, M. and Bax, A. 2001. Characterization of molecular alignment in aqueous suspensions of Pf1 bacteriophage. *J. Biomol. NMR* **20:** 365–377.

Zweckstetter, M., Hummer, G., and Bax, A. 2004. Prediction of charge-induced molecular alignment of biomolecules dissolved in dilute liquid-crystalline phases. *Biophys. J.* **86:** 3444–3460.

Zweckstetter, M., Schnell, J.R., and Chou, J.J. 2005. Determination of the packing mode of the coiled-coil domain of cGMP-dependent protein kinase Iα in solution using charge-predicted dipolar couplings. *J. Am. Chem. Soc.* **127:** 11918–11919.